HHS Public Access

Author manuscript

Mol Cancer Ther. Author manuscript; available in PMC 2017 December 01.

Published in final edited form as:

Mol Cancer Ther. 2016 December ; 15(12): 3064–3076. doi:10.1158/1535-7163.MCT-15-0675.

De-differentiation of glioma cells to glioma stem-like cells by therapeutic stress-induced HIF signaling in the recurrent GBM model

Gina Lee, **Brenda Auffinger**, **Donna Guo**, **Tanwir Hasan**, **Marc Deheeger**, **Alex L Tobias**, **Jeong Yeon Kim**, **Fatemeh Atashi**, **Lingjiao Zhang**[1], **Maciej S. Lesniak**, **James C. David**, and **Atique U. Ahmed**[*]

Department of Neurological Surgery, Northwestern University Feinberg School of Medicine

[1]Department of Surgery, University of Chicago

Abstract

Increasing evidence exposes a subpopulation of cancer cells, known as cancer stem cells (CSCs), to be critical for the progression of several human malignancies, including glioblastoma multiforme (GBM). CSCs are highly tumorigenic, capable of self-renewal, and resistant to conventional therapies, and thus considered to be one of the key contributors to disease recurrence. In order to elucidate the poorly understood evolutionary path of tumor recurrence and the role of CSCs in this process, we developed patient-derived xenograft GBM recurrent models induced by anti-glioma chemotherapy, temozolomide (TMZ). In this model, we observed a significant phenotypic shift towards an undifferentiated population. We confirmed these findings *in vitro* as sorted CD133-negative populations cultured in differentiation-forcing media were found to acquire CD133 expression following chemotherapy treatment. To investigate this phenotypic switch at the single cell level, GSC-specific promoter-based reporter systems were engineered to track changes in the GSC population in real time. We observed the active phenotypic and functional switch of single non-stem glioma cells to a stem-like state and that TMZ therapy significantly increased the rate of single-cell conversions. Importantly, we showed the therapy induced hypoxia inducible factors (HIF) 1α and HIF2α play key roles in allowing non-stem glioma cells to acquire stem-like traits, as the expression of both HIFs increase upon TMZ therapy and knockdown of HIFs expression inhibits the interconversion between non-stem glioma cells and GSCs post-therapy. Based on our results, we propose that anti-glioma chemotherapy promotes the accumulation of HIFs in the GBM cells that induces the formation of therapy-resistant GSCs responsible for recurrence.

[*]To Whom The Reprint Request Should Be Addressed: Department of Neurological Surgery, Northwestern University Feinberg School of Medicine, 303 E. Superior St. Chicago, IL 60611; Tel (312) 503-5978; Fax (312) 503-4855. atique.ahmed@northwestern.edu.

The work of this manuscript dedicated to the memory of Donna Guo.

Disclosure of Potential Conflicts of Interest

The authors declare no competing financial interests

INTRODUCTION

Glioblastoma multiforme (GBM) is the most common adult primary brain tumor and is universally lethal due to its high rate of recurrence (1). Despite aggressive therapeutic intervention, which consists of surgical resection followed by radio and chemotherapy, GBM prognosis remains dismal with less than 10% of patients surviving longer than 5-years after treatment (2, 3). The poor prognosis of GBM results from a high rate of disease recurrence as well as recurrent tumors, which are almost always more aggressive, infiltrative, and therapy-resistant than the original malignancy (4–7). To develop more effective treatments for GBM, it is crucial to understand disease recurrence at the molecular level in order to develop an effective therapeutic strategy to prevent recurrence.

Recent models of tumorigenesis postulate that human malignancies arise from a rare subset of the cancer cells known as cancer stem cells (CSCs), which possess enhanced abilities to self-renew, differentiate and induce the formation of new tumors upon orthotopic implantation in mice (8, 9). It is believed that CSCs possess the inherent capacity to resist conventional therapy and as a result, they play important roles in driving disease recurrence (5, 10). In contrast to traditional models of hierarchical differentiation from the cancer stem cell to differentiated tumor cell populations, recent studies have shown that there exists a dynamic equilibrium between CSC populations and their lineage-committed counterparts (2, 9, 11–13). This equilibrium is regulated by the microenvironmental factors such as intratumoral hypoxia and pH that can influence the rate of tumor differentiation and the balance between asymmetric and symmetric cell division in the CSC compartment and is considered to be critical for disease progression as heterogeneous GBMs contain a small number of glioma stem cells (GSCs) within a larger population of less-tumorigenic differentiated tumor cells (14). Any shift in this equilibrium has the potential to influence clinical outcomes of specific tumors as such shifts may result in a larger number of therapy-resistant CSCs within the tumor that allow them to acquire more aggressive characteristics and to produce poorer prognoses in patients (13, 15). Our laboratory, along with others, has shown that therapeutic stress promotes cellular plasticity, enhancing the conversion of non-stem GBM cells to highly infiltrative, tumor-initiating stem-like cells (16–18). These data argues against the unidirectional flow of cellular hierarchy, increasing the possibility that the fate of these cancer cells is rather a bidirectional, dynamic process (19, 20).

In order to understand how the bidirectional flow of cancer cells influences the stemness equilibrium in GBM during anti-glioma chemotherapy and to elucidate the molecular mechanisms governing such equilibrium, we developed a chemo-induced GBM recurrence model. A shift in the equilibrium towards a more stem-like state was observed in patient-derived GBM tumors (PDX) post-therapy. To examine such conversion dynamics at the single cell level GSC-specific reporter systems using promoter region of multiple GSC-associated genes have been developed, and the conversion was monitored in real time. To further investigate the molecular mechanisms governing such conversion, the HIF-signaling axis has been identified as a key mediator in stimulating the bidirectional conversion of glioma cells, promoting the progression of the recurrent and refractory disease. Unveiling the relationship between therapy-induced HIFs and GSCs allow us to develop therapeutic

strategies that will enhance current standards of care and eliminate the regeneration of recurrent GBM post-therapy.

MATERIALS AND METHODS

Cell culture and propagation

Patient-derived xenograft (PDX) glioma specimens GBM43 and GBM6 were provided by Dr. David James from Northwestern University and maintained according to the published protocol with some modifications (21). For in vitro examination of therapy-induced reprogramming of non-GSC to GSC, the PDX GBM cells were forced into differentiation using 10% FBS containing media. They were modified to constitutively express a blue fluorescent protein (BFP) using lentivirus-mediated infection in culture and then propagated in vivo by serial passaging in flanks of athymic nude mice.

The human glioma cell lines U87 were purchased from the American Type Culture Collection (Manassas, VA, USA) and U251 from Sigma (St. Louis, MO) in 2013. Cells were maintained in culture in Dulbecco's Modified Eagle's Medium (DMEM) with 2 mmol/l L-glutamine (Mediatech, Manassas, VA, USA), 10% fetal bovine serum (FBS; Atlanta Biologicals, Lawrenceville, GA, USA), and 2% penicillin-streptomycin antibiotic (Cellgro, Manassas, VA, USA). Cells were grown in 37°C, and 5% CO2 humidified atmospheric conditions and were enzymatically dissociated using 0.25% trypsin/2.21 mmol/l EDTA solution (Mediatech).

Authentication of PDX and GBM line performed bi-yearly by using Promega GenePrint 10 system, which allowed us to co-amplifies ten human loci (TH01, TPOX, vWA, Amelogenin, CSF1PO, D16S539, D7S829, D13S317, D5S818 and D21S11. The amplified DNA from each cell line was then sent to Northwestern University Sequencing Core Facility. The GeneMapper 5 software was used to analyze raw data that provide us series of DAN sequence that can be compared against a database in Northwestern Nervous System Tissue Bank, ATCC, and Sigma. This test collectively provided a genetic signature with a random match probability of 1 in 2.92 × 109, which exceeds the standards ASN-0002 issued by the American Type Culture Collection Standards Development Organization Workgroup for cell line authentication.

Development of glioma stem cell (GSC)-specific reporter system

GSC-specific promoters – SOX2, Oct4, Nanog, and CD133 – in the Light Switch Promoter Reporter system were obtained from Switchgear Genomics (Cat. No's. S706722, S722579, S722680; Carlsbad, CA, USA). The promoters were subcloned into the pDC516 vector (Cat. No. PD-01-36, Microbix Biosystems Inc., Mississauga, Ontario, Canada) and then inserted into the lentiviral shuttle vector pCMV-RTK upstream of the red fluorescent protein (RFP) gene (Systems Biosciences, Mountain View, GA, USA). Lentiviruses were produced using X293T human embryonic kidney cells for infection according to the published protocol (22). GBM43, U251 and U87 cell lines were simultaneously induced to express the blue fluorescent protein (BFP) using lentivirus-mediated infection in culture and then the populations expressing high-intensity BFP were sorted by FACS.

Animal studies

The recurrent tumor model was developed using PDX models GBM6-BFP and GBM43-BFP. Mice were briefly anesthetized with ketamine (115 mg/kg), and the stereotactic injection was carried out using a 10 μl Hamilton syringe (Reno, NV, USA) with a 30-gauge needle, which was inserted through a burr hole to a depth of 2.5 mm (1000 cells). Five days post-implantation, mice were treated without and with TMZ (2.5 mg/kg/day for 5 days; i.p. injection, n=10); 3 days post-therapy, five mice without and five mice with TMZ were sacrificed, leaving five TMZ-treated mice to be observed and sacrificed upon sickness.

Analysis of GSC-specific promoter activity *in vivo* pre and post-chemotherapy was performed by implanting U87-BFP cells engineered to express a red fluorescent protein (RFP) driven by Oct4, SOX2, CD133, and Nanog promoter into flanks of nude mice. Once the tumors were established mice were treated with TMZ (2.5 mg/kg/day) for 5 days and imaged the same tumor using the two-photon IVM (post-therapy). To investigate the intratumoral localization of the RFP-tagged CSCs, the GBM cells with stably expressing Oct4 reporter system were implanted orthotopically, and a cranial window was placed on the animal brain according to published protocol (23). After two weeks post tumor implantation two-photon intravital microscopy (IVM) was performed to capture RFP fluorescence within the tumor bulk (pre-therapy).

Immunofluorescence analysis using confocal microscopy

GBM43 cells were seeded onto an 8-well glass slide chamber (Cat. No. 1256518, Fisher Scientific). Cells were treated with or without TMZ 50μM for 8 days, fixed with 4% paraformaldehyde, and then stained with primary anti-HIF1α antibody. Animal brains with implanted PDX glioma were removed, frozen in Tissue-Tek O.C.T. Compound (Torrance, CA; Cat. No. 4583), and sectioned for analysis. Nuclei were stained with ProLong Gold Antifade Mountant with DAPI (Cat. No. P-36931, Life Technologies, Carlsbad, CA). Images were captured using Zeiss LSM 510 Confocal Microscope at a magnification of 20× (Carl Zeiss Microscopy, Oberkochen, Germany).

shRNA-mediated knockdown of HIF1α and HIF2α

HIF1α and HIF2α lentiviral shRNA constructs were purchased from Genecopeia (Cat. No. HSH008832-LvU6, HSH005050-LVRU6GP; Rockville, MD, USA) and used to infect U251-blue cells following the lentiviral infection protocol mentioned above. Knockdown efficiency was confirmed by Western Blot and flow cytometry.

Single-cell conversion in real-time

GBM43 and U251-BFP cells with Sox2, Oct4, or Nanog promoters driving RFP expression were plated in 35mm round live-cell dishes on 10mm-diameter glass-bottom insets (MatTek Corporation, Ashland, MA, USA). Cells were treated with TMZ. 72 hours post-treatment, dishes were placed inside the Olympus LCV110U VivaView incubator, which was kept at 37°C/5% CO2 and housed an inverted fluorescence microscope (Olympus, Tokyo, Japan). Images were taken every hour for 24 hours at 20× magnification using MetaMorph image capture software (Olympus) and were analyzed using Fiji image processing program (National Institutes of Health, Bethesda, MA, USA).

Statistical analysis

Experimental data were analyzed using GraphPad Prism Software v4.0 (GraphPad Software, San Diego, CA, USA). Data represent results performed in triplicate. Where applicable, unpaired t-tests and survival analysis were applied. Statistical significance was defined as *P<0.05, **P<0.01, and ***P<0.001.

RESULTS

Cell fate equilibrium shifts toward a more stem-like state following tumor recurrence

To investigate the behavior of the GSCs in recurrent diseases, two recurrent GBM models were developed using the PDX lines GBM6 (Classical, MGMT hypermethylated) and GBM43 (Proneural, MGMT unmethylated) tagged with blue fluorescent protein (BFP) (21, 24, 25). After intracranial implantation of the PDX lines into mice, we mimicked clinical recurrence by treating implanted tumors with alkylating agent TMZ, the current standard chemotherapeutic care for GBM. 2.5 mg/kg of TMZ was administered intraperitoneally every day for five days (Fig. 1A). The treatment decreased the tumor burden by approximately 95%, resulting in an improvement of 13 to 27 days in median survival (Supplementary Fig. 1) as compared to vehicle-treated animals (see Methods Section) (26). However, within three to six weeks after treatment, tumors recurred in 100% of TMZ treated mice.

We could subsequently evaluate the status of GSC populations in tumors of three different groups: vehicle-control untreated animals, animals with primary tumors sacrificed 3 days post-treatment and animals with recurrent tumors as determined by symptoms of disease (Fig. 1A). The GSC populations were evaluated by flow cytometry analysis of two GSC-specific phenotypic markers, CD133, CD15, and one transcription factor SOX2. In GBM6 tumor model, there was a significant increase in CD133+, CD15+, and SOX2+ populations in the recurrent tumors as compared to both the primary and the control tumors (Fig. 1B). The greatest increase was seen in the CD15+ compartment with the CD15+GSC population increasing from 11±2.1% in the control group to 85±2.4% for recurrent tumors ($p<0.0001$, Fig. 1B). As there is considerable controversy over the use of single markers to accurately identify cancer stem cell populations, we verified our results by analyzing GSC populations expressing multiple markers. For GBM6 model, a significant increase was observed in all three double-positive GSC populations, CD133+CD15+ as well as CD133+, and CD15+ cells expressing SOX2 transcription factor, as comparing recurrent tumors to the control and non-recurrent groups (Fig. 1B). The largest increase was observed in the CD133+SOX2+ GSC compartment, with an increase from 28±3.0% in the control group to 83±2.3% for recurrent tumors ($p<0.0001$, Fig. 1B). Based on the expression of stemness markers, some GSC populations decreased slightly, immediately after TMZ-treated primary tumors (3-day post therapy) suggesting that TMZ is perhaps partially capable of depleting the GSC population during initial therapy (Fig. 1B–C). However, for GBM6 model, all recurrent tumors had significantly higher GSC populations than their non-recurrent and non-treated counterparts (Fig. 1B).

The results for the GBM43 model were similar. However, single-marker analysis of GBM43 tumors revealed no significant increases in the CD15+ or SOX2+GSC populations in recurrent tumors. As single marker is not the ideal indicator of GSC populations, the dual-marker analysis was performed, and it was seen that all three double-positive populations, CD133+ and CD15+ expressing GSC specific transcription factor SOX2 as well as the CD133+CD15+, were significantly enriched in recurrent tumors when compared with the control ones (Fig. 1C).

In particular, differences between the two models can be affected when the expansion of the GSC pool occurs, either during or immediately after therapy. Our observation revealed that GBM6 tumors exhibit a significant increase in GSC populations following disease recurrence while GBM43 tumors are more enriched in specific GSCs immediately after primary therapy (Fig. 1B–C). However, the observed increase in GSC populations in both PDX models indicates that tumor recurrence following chemotherapy shifts the equilibrium of glioma cells to a more stem-like state.

To investigate the biological consequence of such equilibrium shift we next created a single cell suspension from two freshly isolated GBM patients samples and exposed to 50μM TMZ or vehicle control for 8 days. After day 8 cells were rechallenged with escalating doses of TMZ to evaluate their ability to resist therapy as well as used in the tumorsphere assay in order to measure the CSC frequency. As demonstrated in Supplementary Fig. 2, exposure to TMZ made both of the tested GBM cells significantly more resistance to TMZ (Supplementary Fig. 2A & B). Moreover, the stemness of both of the cells was significantly enhanced post TMZ exposure as the stem cell frequency was elevated at least 3-folds (Supplementary Fig. 2C & D). Finally, to investigate the tumor engraftment efficiency in vivo, we have treated the U251 cells with 50μM TMZ for 8 days. Next, the CD133+ GSCs and CD133CD15 negative non-GSC glioma cells were sorted out by FACS, intracranially implanted (100 and 1000 cells) in the nude mice and animals were monitored for the endpoint survival. As shown in the table in the Supplementary Fig. 2E, the tumor engraftment capacity of the non-GSC population was significantly enhanced in the TMZ treated groups in both 100 and 1000 cells implanted groups as compared to DMSO-treated control. Based on these data along with our previous published data we conclude that post therapy GBM cells are more resistance to rechallenge and enhanced self-renewing capacity (26).

Development of reporter-based system to monitor cellular plasticity in real time

Next, we set to investigate the role of cellular plasticity in promoting post-therapy glioma stem cell niche. Cellular plasticity is a dynamic process and requires monitoring of the changes in the GSC population over time. It is critical to investigate this process in real time in order to elucidate the conditions under and mechanisms through which this plasticity occurs. Therefore, we set to develop a GSC-specific reporter system to study GBM cells plasticity in realy time. One of the greatest challenges in studying GSCs is selecting the appropriate marker to identify the cancer stem population. To overcome this problem, we have designed multiple reporter systems by using the promoter element of four different CSC-specific genes: CD133, Sox2, Nanog, and Oct4, to ensure that reporter expression is

selectively elevated in the GSCs compartment (Fig. 2A). These promoters were cloned upstream from the red fluorescent protein (RFP). The CD133 is one of the most commonly used markers for glioma stem cells, while the other three genes are known as pluripotency factors, those reported to be also associated with cancer stem cell population (20, 27). These reporter systems were then cloned into a lentivirus system, and viral particles were generated in order to stably modify the GBM cell lines as well as the PDX lines. To investigate if these reporter systems can faithfully identify the GSCs population, total mRNA from each samples were compared with respect to the expression levels of several stemness promoting genes such as Sox2, Oct4, CD133, Noggin, Nestin, Musashi, BIII Tubulin, as well as GFAP mRNA transcripts in the RFP-positive versus RFP negative populations. For CD133-p-RFP reporter cell line, we observed statistically significant upregulation of CD133, SOX2, Oct4 and Noggin mRNA expression in RFP-positive versus RFP negative populations (Fig. 2B1). The RFP-positive population of the Sox2-p-RFP reporter cell line demonstrated statistically significant upregulation of Sox2, Oct4, and Noggin mRNA expression. However, as expected, GFAP transcripts were downregulated. Additionally, no statistically significant difference in CD133, Nestin, Musashi, and B III Tubulin mRNA levels was observed when compared to the RFP negative population (Fig. 2C1). Finally, the Nanog-p-RFP reporter cell line showed statistically significant upregulation of Sox2, Noggin, Nestin, and B III Tubulin mRNA expression in the RFP-positive versus RFP negative population. However, there was no statistically significant difference in CD133, Oct4, Musashi, and GFAP mRNA levels between the two populations (Fig. 2D1). Such discrepancy of gene expression pattern between the different reporter systems is probably due to the reported heterogeneity within the glioma stem cell population (28, 29). In most cases, it is unclear whether phenotypically diverse CSC populations are also functionally distinct. To address this relationship, one needs to use the same tumor (cell) system to simultaneously compare the tumorigenic potential of different subsets. In theory, various CSC populations may or may not be hierarchically organized, analogous to how cancer cells, in general, may be organized. Taken together, we conclude that the RFP-positive cells, in general, were expressing an elevated level of cancer stem cell associated genes.

Next, FACS analysis was performed on the four different cell lines: GBM43 SOX2-p-RFP, U251 SOX2-p-RFP, U251 CD133-p-RFP, and U251 Nanog-p-RFP. The highest RFP-positive population at 18.2 % was observed for U251_CD133-p-RFP cell line (Fig. 2C). The GBM43 SOX2-p-RFP, U251 SOX2-p-RFP and the U251 Nanog-p-RFP express RFP for 10.5%, 8.3% (Fig. 2B, data not shown) and 1.01% (Fig. 2D) respectively. Next, to test if the reporter activity correlates with CD133 positive GSC population, a FACS analysis was conducted to study co-localization of the RFP-expression with the CD133 expression with each of the reporter cell lines. The RFP-positive population of all the reporter cell lines expressed high levels of the CD133 surface protein while the opposite was true for all the RFP negative populations (Supplementary Fig. 3). In all four-reporter systems, the mean fluorescence intensity (MFI) for RFP signal ranged from 150–250 in CD133-negative populations, while the RFP signal increased to 700–1000 MFI on CD133-positive populations ($p<0.0001$, Supplementary Fig. 3).

After examining that the reports systems were capable of identifying GSC subpopulation phenotypically, the functional characteristics of the RFP+ population of cells in vitro were

verified. The RFP-positive and RFP negative populations from the reporter cell lines were sorted out on the BD FACS Aria and subsequently used in a tumorsphere assay to evaluate their stem-like phenotype (Fig. 2B1 & C1). Tumorsphere assay is normally set up in non-adhere 96 well plates to enhance tumor-sphere formation (30). However, the tumorsphere assay was firstly conducted in a coated plate to confirm comparison of RFP expression in the neurosphere-forming cells and the adherent cells (with lower stemness) in one assay. As shown in Fig.2 B2 and C2, glioma cells that were capable of forming neurosphere also express high levels of RFP while the attached cells entirely lost RFP expression indicating that the reporter system did get activated only in the cells that were part of tumorspheres. Next, to investigate in vivo distribution and localization of CSC-specific reporter labeled GSC, the blue fluorescent protein (BFP)-labeled GBM43-Sox2-p-RFP cells were implanted intracranially for eventual imaging by the intravital microscopy. Two-photon intravital microscopy (refer to Materials and Methods section) enable us to image the reporter-induced RFP expression in the BFP positive tumor's anatomy in live animals (Fig. 2E1). Our observation revealed that in the Sox2 reporter tumor, the majority of the RFP-positive cells were localized near the vasculature labeled with the green dextran (Fig. 2E). Thus, our preliminary study suggests that RFP-labeled GSCs demonstrated perivascular niche as described previously in the literature (31). Finally, standard tumorsphere assays were performed in non-coated 96 well plate by plating a different number of sorted RFP-positive and negative cells in the neurosphere media. As demonstrated in Fig 2G and H, the RFP-positive cells exhibited a significantly elevated level of self-renewing ability with cancer stem cell frequency 1 in 214 GBM cells in the RFP-positive population as compared to 1 in 619 population in the RFP negation population for SOX2 reporter cells (Fig. 2G). In the Oct4 reporter cells, the stem cell frequency was 1/189 and 1/554 for RFP-positive and RFP negative cells respectively (Fig. 2H). Collectively, these data indicated that these reporter systems could faithfully detect the GSCs in real time.

Non-stem cancer cells acquire stem-like state post-therapy in the single-cell level

In our recurrent GBM model, we observed a population-wide shift in fate cell equilibrium. To investigate if similar dynamics occur in cell fate equilibrium as of our recurrent GBM model, post therapy stemness was monitored at the single-cell level. First, to confirm our in vivo findings of glioma cell "de-differentiation" in vitro, the GBM43 PDX line was treated with either 50μM TMZ, the maximum concentration found in human blood plasma (32, 33), or vehicle treated control (DMSO). The cells were sorted by flow cytometry for stem-like CD133+ and non-stem CD133− populations of each group (14). The sorted populations were cultured in fetal bovine serum (FBS), which forces differentiation in order to minimize contamination with the CSC populations during sorting (Supplementary Fig. 4) (18). In this condition the GSC CD133 expressing as well as CD133 negative non-GSC populations were sorted every 48 hours for 20 days in the presence or absence of TMZ (Fig. 3A). For a baseline control, the untreated CD133− and CD133+ populations were sorted. Both populations together with an unsorted ("DMSO") population reached an equilibrium percentage of 1–2% CD133+ cells within 48–72 hours (Fig. 3A). When cells were pre-treated with DMSO or TMZ before sorting, all DMSO-treated cell populations returned to baseline levels within 72 hours regardless of their initial percentage after sorting (Fig. 3A). Approximately 1–2% of sorted CD133− populations started to expressed CD133 within 48

hours, while the sorted CD133+ population lost CD133 expression to reach an equilibrium of 1–2% 72 hours post-sorting (Fig. 3A).

In contrast, TMZ-treated sorted cell populations showed a significant change from baseline levels (Fig. 3A). The sorted TMZ treated CD133+ population took approximately 10 days to reach the equilibrium, and the percent of CD133+GSCs was about 16%, which is about 9-fold higher than the control (Fig. 3A). In the sorted CD133− population treated with TMZ, cells immediately increased in CD133 protein expression, reached a peak at day six (14% ±1), and then decreased at days eight to ten, maintaining their downhill trend until 20 days post-sorting. This in vitro observation, therefore, confirmed results of in vivo observations, which helped us conclude that TMZ-therapy shifts the equilibrium proportion of GSCs in tumor cell populations both in vivo and in-vitro.

To further investigate this phenomenon of cellular plasticity at the single-cell level and its contribution to cell fate equilibrium shift post therapy, GSC-specific reporter systems were employed to track interconversion between glioma stem and non-stem cells. GBM43 and U251 GBM cells stably expressing GSC-specific reporters were subsequently cultured in the presence or absence of TMZ for 8 days and analyzed by flow cytometry to determine whether the cells with active promoters also expressed GSC-specific phenotypic markers as well as reprogramming transcription factors. Single-cell analysis of engineered cells using Olympus VivaView real-time sequential imaging showed active conversions of previously RFP− cells (non-GSCs) into RFP+ cells (GSCs) in chemotherapy-treated samples 4–6 days post-therapy (Figs. 3B–C). The percentage of RFP-positive GBM43 cells expressing SOX2-p-RFP was consistently and significantly lower compared to TMZ-treated cells (9.34%±0.81 vs. 17.91%±1.29, $p<0.001$). For U251 cells expressing SOX2-p-RFP, the percentage of RFP-positive was consistently and significantly lower compared to TMZ-treated cells (14%±2.2 vs. 35%±5.3, $p<0.001$). A very similar result was also observed by using Oct4− and Nanog− reporter systems (Supplementary Fig. 5 A, B & C). Baseline spontaneous conversion rates of 14% for RFP+Sox2-tagged, 11% for RFP+Oct4-tagged, and 22% for RFP+Nanog-tagged GBM fell within the range of Sox2+, Oct4+, and Nanog+ glioma cells reported by other groups (26, 34, 35). After chemotherapy treatment, the frequency of RFP negative cells (RFP−) cells that became RFP-positive (RFP+) increased to approximately 35%, 36%, and 43% for Sox2, Oct4, and Nanog promoters, respectively ($p<0.01$). Next, to examine if these post therapy RFP-positive cells also express other GSC-specific markers, the TMZ treated U251 CD133-p-RFP cells were FACS analyzed (Fig. 3D). In this reporter system, a majority of the post therapy RFP-positive cells were significantly colocalized with the CD133, CD15, and SOX2 expressing GBM cells. Similar experiments were performed with the other three reporter systems, which demonstrated that post-therapy RFP+ cells were also expressing GSC-specific markers such as CD133 and SOX2 (Fig. 3E and Supplementary Fig. 5D).

Next, to validate these observations in vivo, the GBM cells expressing RFP driven by Oct4 promoter were implanted intracranially, and once the tumor was engrafted, the RFP+ tumor cells within the tumor bulk were detected by using cranial window and intravital microscopy (IVM). The tumor-bearing mice were then treated with chemotherapy for 5 days, and a visually significant increase in RFP expression scattered throughout the tumor bulk within the same animal was observed (Fig. 3F).

Finally, to investigate whether the observed expansion of CD133 population post therapy is not due to proliferation of this specific subpopulation, the CD133− and CD133+ populations were examined for their proliferative capacity post therapy by Ki67 staining (Supplementary Fig. 5 E & F). As demonstrated, the TMZ treatment significantly decreased the Ki67 total protein expression as well as the percent of Ki67 positive cells, only in the CD133+ GSC compartment. This data indicated that the observed post therapy induced expansion of the GSC compartment is not due to the proliferation of the CD133+ GSCs. Next, to investigate if the post-therapy induced GSCs can be differentiated into the different, previously reported differentiation inducing agent bone morphogenic protein 2 (BMP2) was added at day 6 post TMZ treatment for 2 days (36). These cells were subsequently analyzed by FACS and observed that in the presence of BMP2, the TMZ induced GSCs in the GBM43 PDX line cultured in serum free neurobasal media (Supplementary Fig. 6A & B) or in the FBS containing media (Supplementary. Fig. 6C & D) significantly decreased the GSC-specific markers such as CD133 and CD15 as well as upregulation of astrocytic lineage marker GFAP. These data is another validation of the CSC authenticity of the therapy induced GSCs. Taken together, these data showed that GSC-specific promoter activities, as well as GSC-specific phenotypic markers, were significantly enhanced during primary chemotherapy. This real-time observation of cellular plasticity at the population level combining with our functional data positively indicated the ability of non-GSCs to acquire GSC-like states in the presence of therapeutic stress.

HIF1α mediates the conversion of non-stem glioma cells into GSCs

Cellular responses to hypoxia are commonly regulated by hypoxia-inducible factors (HIFs), which are key transcriptional factors active in the cell during oxygen tension. Our previous report indicated that anti-glioma chemotherapy induces the expression of HIFs and promotes hypoxia-like responses (26) and the intratumoral hypoxia niche was previously described as an important factor for the maintenance of the GSC subpopulation found within glioma (27, 37, 38). Based on this reasoning, the role of therapy-induced HIFs in regulating the equilibrium of cellular stemness during anti-glioma therapy was investigated.

Examining the levels of both HIF1α and HIF2α in a GBM model after primary chemotherapy, a significant increase in levels of HIF1α and HIF2α expressions was observed in cells treated with TMZ (50μM) as compared to the control (Fig. 4A). HIF1α expression was consistently elevated in chemotherapy-treated samples from day two through eight. On day two, HIF1α MFI was 845±1.5 for DMSO-treated and 1190±2.2 for TMZ-treated ($p<0.001$), while on day eight MFI levels were almost the same at 820±1.2 for DMSO-treated and 1100±2.7 for TMZ treated ($p<0.001$) (Fig. 4A). While HIF2α expression was similarly elevated in TMZ-treated conditions as compared to control, the HIF2α increased over time and reached its peak 6–8 days after primary therapy. On day two, HIF2α MFI for DMSO-treated was 248±0.4 and 375±0.6 for TMZ-treated, and on day eight, MFI for TMZ-treated samples increased to 730±4.7 with DMSO at 252±0.2 ($p<0.001$) (Fig. 4A).

This result opens a new insight into the dynamics of HIF transcriptional factors in the hypoxic microenvironment. The HIF1α transcriptional factor is expressed immediately after the oxygen tension is initiated, and HIF2α is expressed at the chronic phase of hypoxia (39).

Based on our data, we propose that the immediate peak expression of HIF1α in PDX GBM cells after exposure to chemotherapy may represent one of the necessary steps for the conversion of non-GSCs into GSCs. Meanwhile, the increase in HIF2α expression over an extended period may be required for the maintenance of the newly converted GSCs post therapy.

To further evaluate the dynamics of chemotherapy-induced HIF activation, an HIF1α-responsive reporter assay was utilized (Fig. 4B). In order to stabilize itself, HIFα dimerizes with HIFβ and then binds to hypoxia-responsive elements (HREs) located in the promoters of hypoxia-regulated genes. The subsequent binding activates the transcription of in numerous genes responsible for modulating cell survival and metabolism (40).

The functionality and physiological relevance of the increase in HIF activity after chemotherapy were investigated by analyzing in vivo expressions of HIF1α and HIF2α in the PDX GBMs at 3 days post-primary chemotherapy as well as upon tumor recurrence (Fig. 5A & B). Experiments were performed in the recurrent model as described in Fig. 1 in two different PDX lines (GBM43 proneural and GBM6 classical). The GBM43 model presented a significantly higher expression of HIF1α at 3 days post-primary chemotherapy as compared to the control (Figs. 5A). There was a significant increase in the expressions of HIF1α and HIF2α in the CD133+ GSC compartment both post-therapy and at disease recurrence ($p<0.001$). In the GBM6 PDX model, a higher expression of HIF1α was seen 3 days post-therapy, while HIF2α expression present in the GSC compartment was only observed when the disease recurred.

To further assess the roles of HIF1α and HIF2α in the conversion of non-GSCs into GSCs, shRNA-mediated knockdown of HIF1α or HIF2α in the cancer cells was used (Supplementary Fig. 7). Knockdown of both HIF1α and HIF2α resulted in a three-fold decrease in the CD133+GSC population as compared to control cells ($p<0.001$, Fig. 6A). These findings were confirmed using a chemical inhibitor of HIF1α translation (Calbiochem, 400088) (Fig. 6B). Using a concentration of inhibitor that was not toxic to cells (IC50 of 20μM or lower as determined by 7-AAD staining), the PDX lines were concurrently treated with TMZ and HIF1α inhibitor. As a result, HIF1α inhibition significantly blocked the amplification of CD133+, CD15+, Sox2+, CD133+Sox2+, and CD133+CD15+ GSCs after primary therapy ($p<0.001$). Collectively both HIF1α and HIF2α are critical for conversion of non-GSCs to a GSC-like state post anti-glioma chemotherapy.

DISCUSSION

Despite the standard use of a combination of aggressive therapies (surgical resection followed by chemotherapy and radiation), GBM tumors invariably recur (41, 42). The implementation of temozolomide has only improved the overall survival from 12 to 14.6 months in the clinical setting (2, 42). It is believed that a small population of cells within GBMs, known as glioma stem cells, is responsible for such a dismal disease prognosis (43, 44). The GSCs have the capacity to self-renew, differentiate and give rise to a whole new heterogeneous tumor, and recent reports have demonstrated the existence of both spontaneous and therapy-induced GSC plasticity (15, 17, 26). This open up the possibility of

such bi-directional conversion may preclude optimal efficacies of standard therapies for two main reasons (17, 20, 26, 45). First, as standard therapies mostly target rapidly dividing GBM cells, the subpopulation of quiescent GSCs may largely spared, which leads to a more aggressive recurrent tumor driven by chemotherapy-resistant GSCs (46). Second, due to the invariable interconversion of non-GSGs to GSCs following therapeutic stress, aggressive therapeutic strategies that remove the majority of the tumor bulk and then target the GSC subpopulation are still doomed to fail. The increased occurrence of plasticity between non-GSCs and GSCs during and post-therapy will result in the replenishment of all GBM subpopulations and consequent tumor regrowth (17, 20, 26, 47). In this paper, our main goal is to investigate the dynamics of interconversion during therapy and understand the possible mechanisms behind this conversion process in the recurrent PDX glioma model. To avoid such risks of any contamination of small fraction of CD133+ cells during FACS sorting or quiescent CSCs, which may yet to express phenotypic markers for CSC, we have utilized culture condition media with 10% FBS as well as in the presence of differentiation promoting factor BMP2 that reported promoting differentiation in the CSCs population. In this manuscript, we demonstrate an increased interconversion of non-GSCs to GSCs even in the presence of differentiation condition in vitro as well as in the recurrent model in vivo. The understudied nature of cell fate equilibrium in recurrent GBM allowed us to investigate the dynamics of inherent cellular behavior in response to primary chemotherapy (48), and we found that although cells acquire an equilibrium state over time both in the absence and presence of chemotherapy, there is a distinct shift in the equilibrium of therapy-treated cells to become more stem-like in behavior. Acquiring Stem- like phenotype could be partially due to induction of stem phenotype by chemotherapy or by enhancing the transition of cell status from non-GSC to GSC phenotype. These observations were confirmed by analysis of the whole GBM population as well as on the single-cell level by the development of multiple specific GSC-specific promoter-based reporter systems. Taken together, our results strongly support the concept that the plastic nature of GBM cells promotes their acquisition of stem-like phenotypes post-therapy in addition to highly aggressive malignant characteristics. Further analysis have to be done in the future to determine if any GSC markers or molecular characteristics could be utilize to discriminate tumor forming versus non-tumor forming cells. Also in accordance with previous publications (14, 49–51), we found that different subtypes of GBM present variable responses to initial therapeutic insult. This is mostly seen as varied influences between self-renewal of GSCs and conversion of non-GSCs into GSCs in the recurrent model. The variability between the two models suggests that the unique genetic signature and origin of each PDX model—GBM6 is of classical origin, while GBM43 is proneural—affects their response to therapy (24, 50). For examples, classical subtype of GBM contain EGFR alteration as compared to PDEGR alteration predominately observed in the proneural GBM (50). Therefore, each subtype may respond differently to treatment, such as in the timing of GSC expansion, which can occur during the course of therapy, post-therapy, or as the disease burden progresses and promotes recurrence.

The importance of environmental cues as triggers for the activation of self-renewal in GSCs is undeniable. Data presented in this manuscript indicated that therapy-induced plasticity in the GSC population was at least in part HIF-mediated. Direct measurement of the percentages of HIF1α- and HIF2α-expressing cells in the whole recurrent tumor and

assessment of the activities of both HIFs in CD133+ GSCs revealed that HIF2α had a direct effect on the maintenance of the GSC phenotype while HIF1α was mostly related to the initial activation of this plastic phenomenon. Blocking HIF1α activity using shRNA and a translation inhibitor led to significant decreases in the GSC population after primary chemotherapy. Based on these results, we identified HIF1α as the critical regulator of GBM cell plasticity in our recurrent model. We were able to demonstrate that dedifferentiation of tumor cells by TMZ-induced therapeutic stress is partly mediated by HIFs. The role of HIFs promoting GBM cells stemness has been extensively examined (37, 52). However, some conflicting results have been reported regarding the role of intratumoral hypoxia-mediated CSC niche regulating the chemoresistance properties of GBM. Pistollato et al. investigated the effects of the intratumoral hypoxia gradient on the TMZ resistance capacity of GSC and reported that GSCs located within the core of the tumor were highly resistance to TMZ therapy as compared to GSCs from the tumor periphery. The CD133 expressing cancer cells mostly enriched in the tumor core also overexpress MGMT, a genes that is known be critical for TMZ resistance (53). In a contesting study, Glas et al. demonstrated that even though a fraction of tested CSC lines derived from the core and the periphery of the same patient's GBM tumors responded differentially to radiation, TMZ and CNU, the difference was not consistent in between patients (54). The intratumoral hypoxia has been already linked to chemo- and radioresistant properties of tumor cells as hypoxic niche may reduce the oxidative DNA damage and allow the tumor cells to overcome the conventional radio- and chemotherapy (55). However, the link between hypoxia regulate CSC niche and post therapy GBM recurrence is much more complex than expected as the majority of the GBM patient relapse even after the resection of the entire primary tumor mass including the core of the tumor burden that contains the majority of the hypoxic region (52). Data presented in this manuscript indicated that therapeutic stress could promote hypoxia-like response, which could be independent of intratumoral hypoxia (19, 26). Additional investigation will require elucidating the role of intratumoral hypoxia in post-therapy HIFs accumulation. Collectively, our data suggest that blocking GBM cell plasticity that allows the GBM cells to acquire CSC-like state during chemotherapy can be a potential therapeutic strategy to be used in combination with the standard of care to decrease malignant relapse.

There may be some limitations to our study. First, we have presented limited data regarding the functional aspect of the therapy induced GSCs. Even though we have demonstrated that our GSC-specific reporter systems could faithfully identify the GSC population in real time as the RFP-positive population showed significantly elevated level of self-renewing capacity as compared to RTK-negative cells, in the future, it would be prudent to validating this observation *in vivo* by using a limited dilution tumor formation assay. Secondly, we observed phenotypic heterogeneity within the induced GSC subpopulations. However, the functional characterization of the phenotypic heterogeneity or their contribution to disease recurrence is remaining largely unknown. A negative selection system regulated by our GSC-specific reported system could be employed to address this critical question. Finally, the contribution of intratumoral hypoxia in a post-therapy conversion of GBM cells to GSCs is yet to be investigated. Although our results demonstrated that therapy-induced GSCs niche is independent of the intratumoral hypoxia as therapeutic stress induced HIF expression in the normoxic condition *in vivo*, further studies are required to elucidate the

precious molecular mechanism therapy induced cellular plasticity and its role in disease recurrence.

Cancer cells within individual tumors exist in many distinct phenotypic states that vary significantly with respect to functional characteristics. The diverse cell populations within different tumors usually display a unique equilibrium of cells in various fate states. Such dynamic equilibrium is achieved by the cell fate decision orchestrated by interactions between an individual cell and its microenvironment. This is significant in disease progression because microenvironmental changes, such as extracellular stress, can directly influence survival fitness. As a summary, our results demonstrated that therapeutic stress can shift the intratumoral balance towards a more stem-like state by promoting bi-directional interconvertibility between non-CSC and CSC compartments, possibly promoting an aggressive and therapy-resistant phenotype in recurrent GBM. Elucidating the molecular mechanisms maintaining the intratumoral cell fate equilibrium state and the effects of anti-glioma therapies on the CS niche, gives a new insight to understand how CSCs contribute to disease progression, identify novel therapeutic targets to prevent GBM recurrence, and promote a better prognosis for GBM patients in the future.

Supplementary Material

Refer to Web version on PubMed Central for supplementary material.

Acknowledgments

Financial Support: This work was supported by the National Cancer Institute grant R00 CA160775 and the American Cancer Society (299503) grant (A.U. Ahmed).

We thank Dr. Mejing Wu for her statistical assistance.

References

1. Wen PY, Kesari S. Malignant gliomas in adults. The New England journal of medicine. 2008; 359:492–507. [PubMed: 18669428]
2. Stupp R, Mason WP, van den Bent MJ, Weller M, Fisher B, Taphoorn MJ, et al. Radiotherapy plus concomitant and adjuvant temozolomide for glioblastoma. The New England journal of medicine. 2005; 352:987–996. [PubMed: 15758009]
3. Anton K, Baehring JM, Mayer T. Glioblastoma multiforme: overview of current treatment and future perspectives. Hematology/oncology clinics of North America. 2012; 26:825–853. [PubMed: 22794286]
4. Mangiola A, de Bonis P, Maira G, Balducci M, Sica G, Lama G, et al. Invasive tumor cells and prognosis in a selected population of patients with glioblastoma multiforme. Cancer. 2008; 113:841–846. [PubMed: 18618580]
5. Chen R, Nishimura MC, Bumbaca SM, Kharbanda S, Forrest WF, Kasman IM, et al. A hierarchy of self-renewing tumor-initiating cell types in glioblastoma. Cancer cell. 2010; 17:362–375. [PubMed: 20385361]
6. Bambury RM, Morris PG. The search for novel therapeutic strategies in the treatment of recurrent glioblastoma multiforme. Expert review of anticancer therapy. 2014; 14:955–964. [PubMed: 24814143]
7. Kamiya-Matsuoka C, Gilbert MR. Treating recurrent glioblastoma: an update. CNS oncology. 2015; 4:91–104. [PubMed: 25768333]

8. Singh SK, Clarke ID, Terasaki M, Bonn VE, Hawkins C, Squire J, et al. Identification of a cancer stem cell in human brain tumors. Cancer research. 2003; 63:5821–5828. [PubMed: 14522905]
9. Singh SK, Hawkins C, Clarke ID, Squire JA, Bayani J, Hide T, et al. Identification of human brain tumour initiating cells. Nature. 2004; 432:396–401. [PubMed: 15549107]
10. Ben-Porath I, Thomson MW, Carey VJ, Ge R, Bell GW, Regev A, et al. An embryonic stem cell-like gene expression signature in poorly differentiated aggressive human tumors. Nature genetics. 2008; 40:499–507. [PubMed: 18443585]
11. O'Brien CA, Pollett A, Gallinger S, Dick JE. A human colon cancer cell capable of initiating tumour growth in immunodeficient mice. Nature. 2007; 445:106–110. [PubMed: 17122772]
12. Patrawala L, Calhoun T, Schneider-Broussard R, Li H, Bhatia B, Tang S, et al. Highly purified CD44+ prostate cancer cells from xenograft human tumors are enriched in tumorigenic and metastatic progenitor cells. Oncogene. 2006; 25:1696–1708. [PubMed: 16449977]
13. Iliopoulos D, Hirsch HA, Wang G, Struhl K. Inducible formation of breast cancer stem cells and their dynamic equilibrium with non-stem cancer cells via IL6 secretion. Proceedings of the National Academy of Sciences of the United States of America. 2011; 108:1397–1402. [PubMed: 21220315]
14. Sturm D, Witt H, Hovestadt V, Khuong-Quang DA, Jones DT, Konermann C, et al. Hotspot mutations in H3F3A and IDH1 define distinct epigenetic and biological subgroups of glioblastoma. Cancer cell. 2012; 22:425–437. [PubMed: 23079654]
15. Chaffer CL, Brueckmann I, Scheel C, Kaestli AJ, Wiggins PA, Rodrigues LO, et al. Normal and neoplastic nonstem cells can spontaneously convert to a stem-like state. Proceedings of the National Academy of Sciences of the United States of America. 2011; 108:7950–7955. [PubMed: 21498687]
16. Auffinger B, Ahmed AU, Lesniak MS. Oncolytic virotherapy for malignant glioma: translating laboratory insights into clinical practice. Frontiers in oncology. 2013; 3:32. [PubMed: 23443138]
17. Dahan P, Martinez Gala J, Delmas C, Monferran S, Malric L, Zentkowski D, et al. Ionizing radiations sustain glioblastoma cell dedifferentiation to a stem-like phenotype through survivin: possible involvement in radioresistance. Cell death & disease. 2014; 5:e1543. [PubMed: 25429620]
18. Fessler E, Borovski T, Medema JP. Endothelial cells induce cancer stem cell features in differentiated glioblastoma cells via bFGF. Molecular cancer. 2015; 14:157. [PubMed: 26282129]
19. Deheeger M, Lesniak MS, Ahmed AU. Cellular plasticity regulated cancer stem cell niche: a possible new mechanism of chemoresistance. Cancer cell & microenvironment. 2014:1.
20. Safa AR, Saadatzadeh MR, Cohen-Gadol AA, Pollok KE, Bijangi-Vishehsaraei K. Glioblastoma stem cells (GSCs) epigenetic plasticity and interconversion between differentiated non-GSCs and GSCs. Genes & Diseases. 2015; 2:152–163. [PubMed: 26137500]
21. Kitange GJ, Carlson BL, Schroeder MA, Grogan PT, Lamont JD, Decker PA, et al. Induction of MGMT expression is associated with temozolomide resistance in glioblastoma xenografts. Neuro-oncology. 2009; 11:281–291. [PubMed: 18952979]
22. Tiscornia G, Singer O, Verma IM. Production and purification of lentiviral vectors. Nature protocols. 2006; 1:241–245. [PubMed: 17406239]
23. Orringer DA, Chen T, Huang DL, Armstead WM, Hoff BA, Koo YE, et al. The brain tumor window model: a combined cranial window and implanted glioma model for evaluating intraoperative contrast agents. Neurosurgery. 2010; 66:736–743. [PubMed: 20305495]
24. Sarkaria JN, Carlson BL, Schroeder MA, Grogan P, Brown PD, Giannini C, et al. Use of an orthotopic xenograft model for assessing the effect of epidermal growth factor receptor amplification on glioblastoma radiation response. Clinical cancer research : an official journal of the American Association for Cancer Research. 2006; 12:2264–2271. [PubMed: 16609043]
25. Verhaak RG, Hoadley KA, Purdom E, Wang V, Qi Y, Wilkerson MD, et al. Integrated genomic analysis identifies clinically relevant subtypes of glioblastoma characterized by abnormalities in PDGFRA, IDH1, EGFR, and NF1. Cancer cell. 2010; 17:98–110. [PubMed: 20129251]
26. Auffinger B, Tobias AL, Han Y, Lee G, Guo D, Dey M, et al. Conversion of differentiated cancer cells into cancer stem-like cells in a glioblastoma model after primary chemotherapy. Cell death and differentiation. 2014; 21:1119–1131. [PubMed: 24608791]

27. Huang Z, Cheng L, Guryanova OA, Wu Q, Bao S. Cancer stem cells in glioblastoma--molecular signaling and therapeutic targeting. Protein Cell. 2010; 1:638–655. [PubMed: 21203936]
28. Hubert CG, Rivera M, Spangler LC, Wu Q, Mack SC, Prager BC, et al. A Three-Dimensional Organoid Culture System Derived from Human Glioblastomas Recapitulates the Hypoxic Gradients and Cancer Stem Cell Heterogeneity of Tumors Found In Vivo. Cancer research. 2016; 76:2465–2477. [PubMed: 26896279]
29. Natsume A, Ito M, Katsushima K, Ohka F, Hatanaka A, Shinjo K, et al. Chromatin regulator PRC2 is a key regulator of epigenetic plasticity in glioblastoma. Cancer research. 2013; 73:4559–4570. [PubMed: 23720055]
30. Azari H, Millette S, Ansari S, Rahman M, Deleyrolle LP, Reynolds BA. Isolation and expansion of human glioblastoma multiforme tumor cells using the neurosphere assay. Journal of visualized experiments : JoVE. 2011:e3633. [PubMed: 22064695]
31. Calabrese C, Poppleton H, Kocak M, Hogg TL, Fuller C, Hamner B, et al. A perivascular niche for brain tumor stem cells. Cancer cell. 2007; 11:69–82. [PubMed: 17222791]
32. Brada M, Judson I, Beale P, Moore S, Reidenberg P, Statkevich P, et al. Phase I dose-escalation and pharmacokinetic study of temozolomide (SCH 52365) for refractory or relapsing malignancies. British journal of cancer. 1999; 81:1022–1030. [PubMed: 10576660]
33. Beier D, Rohrl S, Pillai DR, Schwarz S, Kunz-Schughart LA, Leukel P, et al. Temozolomide preferentially depletes cancer stem cells in glioblastoma. Cancer research. 2008; 68:5706–5715. [PubMed: 18632623]
34. Bier A, Giladi N, Kronfeld N, Lee HK, Cazacu S, Finniss S, et al. MicroRNA-137 is downregulated in glioblastoma and inhibits the stemness of glioma stem cells by targeting RTVP-1. Oncotarget. 2013; 4:665–676. [PubMed: 23714687]
35. Silvestri I, Testa F, Zappasodi R, Cairo CW, Zhang Y, Lupo B, et al. Sialidase NEU4 is involved in glioblastoma stem cell survival. Cell death & disease. 2014; 5:e1381. [PubMed: 25144716]
36. Schneider L, Pellegatta S, Favaro R, Pisati F, Roncaglia P, Testa G, et al. DNA damage in mammalian neural stem cells leads to astrocytic differentiation mediated by BMP2 signaling through JAK-STAT. Stem cell reports. 2013; 1:123–138. [PubMed: 24052948]
37. Li Z, Bao S, Wu Q, Wang H, Eyler C, Sathornsumetee S, et al. Hypoxia-inducible factors regulate tumorigenic capacity of glioma stem cells. Cancer cell. 2009; 15:501–513. [PubMed: 19477429]
38. Mathew LK, Skuli N, Mucaj V, Lee SS, Zinn PO, Sathyan P, et al. miR-218 opposes a critical RTK-HIF pathway in mesenchymal glioblastoma. Proceedings of the National Academy of Sciences of the United States of America. 2014; 111:291–296. [PubMed: 24368849]
39. Menrad H, Werno C, Schmid T, Copanaki E, Deller T, Dehne N, et al. Roles of hypoxia-inducible factor-1alpha (HIF-1alpha) versus HIF-2alpha in the survival of hepatocellular tumor spheroids. Hepatology. 2010; 51:2183–2192. [PubMed: 20513003]
40. Harris AL. Hypoxia--a key regulatory factor in tumour growth. Nat Rev Cancer. 2002; 2:38–47. [PubMed: 11902584]
41. Legler JM, Ries LA, Smith MA, Warren JL, Heineman EF, Kaplan RS, et al. Cancer surveillance series [corrected]: brain and other central nervous system cancers: recent trends in incidence and mortality. Journal of the National Cancer Institute. 1999; 91:1382–1390. [PubMed: 10451443]
42. Stupp R, Hegi ME, Mason WP, van den Bent MJ, Taphoorn MJ, Janzer RC, et al. Effects of radiotherapy with concomitant and adjuvant temozolomide versus radiotherapy alone on survival in glioblastoma in a randomised phase III study: 5-year analysis of the EORTC-NCIC trial. Lancet Oncol. 2009; 10:459–466. [PubMed: 19269895]
43. Galli R, Binda E, Orfanelli U, Cipelletti B, Gritti A, De Vitis S, et al. Isolation and characterization of tumorigenic, stem-like neural precursors from human glioblastoma. Cancer research. 2004; 64:7011–7021. [PubMed: 15466194]
44. Yuan X, Curtin J, Xiong Y, Liu G, Waschsmann-Hogiu S, Farkas DL, et al. Isolation of cancer stem cells from adult glioblastoma multiforme. Oncogene. 2004; 23:9392–9400. [PubMed: 15558011]
45. Wang J, Sakariassen PO, Tsinkalovsky O, Immervoll H, Boe SO, Svendsen A, et al. CD133 negative glioma cells form tumors in nude rats and give rise to CD133 positive cells. International journal of cancer Journal international du cancer. 2008; 122:761–768. [PubMed: 17955491]

46. Inda MM, Bonavia R, Mukasa A, Narita Y, Sah DW, Vandenberg S, et al. Tumor heterogeneity is an active process maintained by a mutant EGFR-induced cytokine circuit in glioblastoma. Genes & development. 2010; 24:1731–1745. [PubMed: 20713517]

47. Chaffer CL, Marjanovic ND, Lee T, Bell G, Kleer CG, Reinhardt F, et al. Poised chromatin at the ZEB1 promoter enables breast cancer cell plasticity and enhances tumorigenicity. Cell. 2013; 154:61–74. [PubMed: 23827675]

48. Yang S, Cohen CJ, Peng PD, Zhao Y, Cassard L, Yu Z, et al. Development of optimal bicistronic lentiviral vectors facilitates high-level TCR gene expression and robust tumor cell recognition. Gene therapy. 2008; 15:1411–1423. [PubMed: 18496571]

49. Phillips HS, Kharbanda S, Chen R, Forrest WF, Soriano RH, Wu TD, et al. Molecular subclasses of high-grade glioma predict prognosis, delineate a pattern of disease progression, and resemble stages in neurogenesis. Cancer cell. 2006; 9:157–173. [PubMed: 16530701]

50. Verhaak RG, Hoadley KA, Purdom E, Wang V, Qi Y, Wilkerson MD, et al. Integrated genomic analysis identifies clinically relevant subtypes of glioblastoma characterized by abnormalities in PDGFRA, IDH1, EGFR, and NF1. Cancer cell. 2010; 17:98–110. [PubMed: 20129251]

51. Mao P, Joshi K, Li J, Kim SH, Li P, Santana-Santos L, et al. Mesenchymal glioma stem cells are maintained by activated glycolytic metabolism involving aldehyde dehydrogenase 1A3. Proceedings of the National Academy of Sciences of the United States of America. 2013; 110:8644–8649. [PubMed: 23650391]

52. Persano L, Rampazzo E, Basso G, Viola G. Glioblastoma cancer stem cells: role of the microenvironment and therapeutic targeting. Biochemical pharmacology. 2013; 85:612–622. [PubMed: 23063412]

53. Pistollato F, Abbadi S, Rampazzo E, Persano L, Della Puppa A, Frasson C, et al. Intratumoral hypoxic gradient drives stem cells distribution and MGMT expression in glioblastoma. Stem cells. 2010; 28:851–862. [PubMed: 20309962]

54. Glas M, Rath BH, Simon M, Reinartz R, Schramme A, Trageser D, et al. Residual tumor cells are unique cellular targets in glioblastoma. Annals of neurology. 2010; 68:264–269. [PubMed: 20695020]

55. Keith B, Simon MC. Hypoxia-inducible factors, stem cells, and cancer. Cell. 2007; 129:465–472. [PubMed: 17482542]

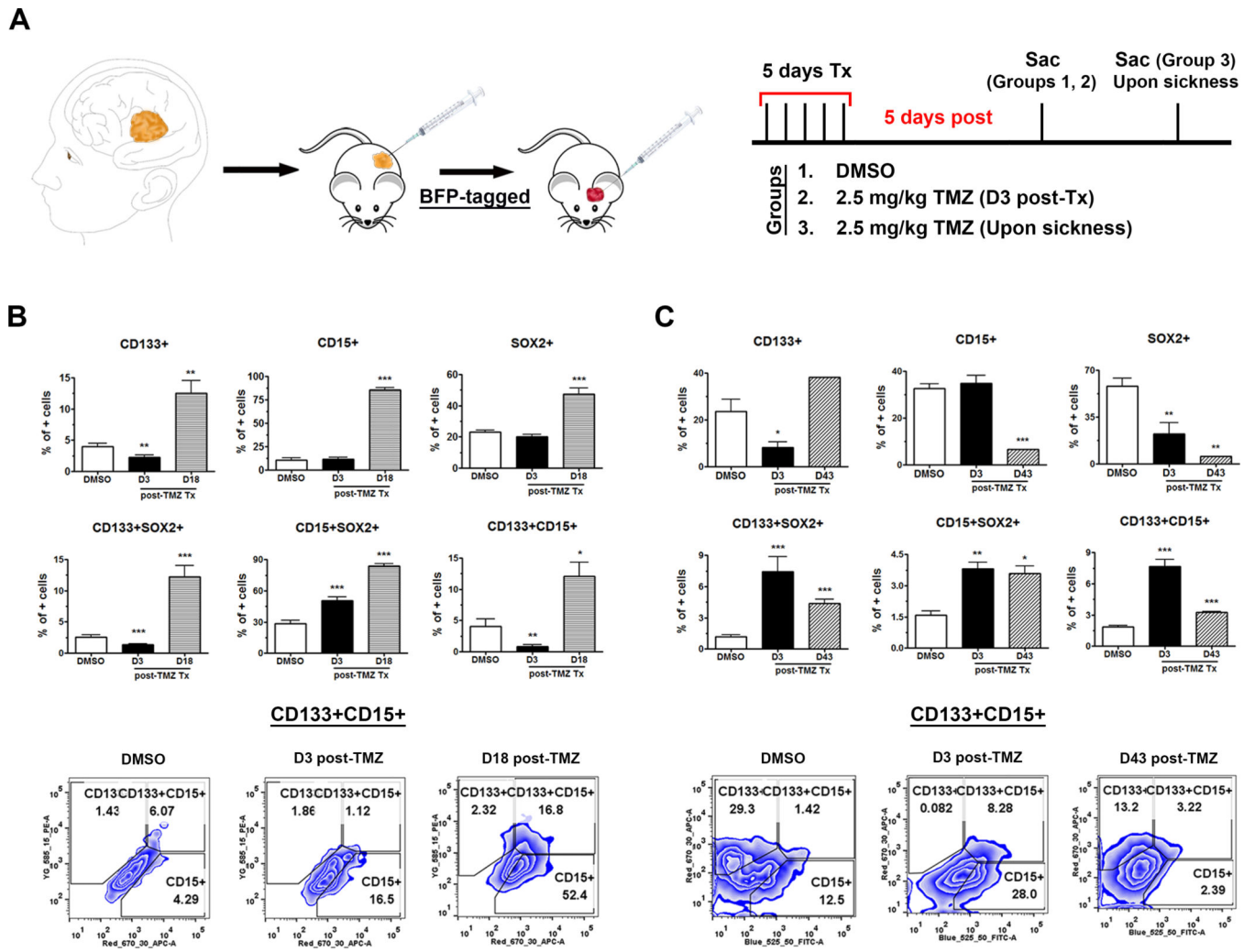

Figure 1. Cell fate equilibrium shifted toward a more stem-like state in the GBM recurrent model

A) Schematic of the establishment of GBM recurrence model. B, C) There is an increased expression of various GSC subpopulations in GBM6 (B) and GBM43 (C) blue-tagged tumors, respectively, after primary chemotherapy (TMZ 2.5 mg/kg for 5 days treatment). PDX lines were implanted orthotopically and waited for 5 to 10 days for xenograft establishment. A dose of 2.5 mg/kg/day of TMZ was administering intraperitoneally for 5 days in tumor-bearing mice. We evaluated the status of the GSC population using flow cytometry in our animal groups: untreated vehicle, sacrificed 3 days post-completion of chemotherapy, and upon disease recurrence (determined by symptoms of disease). GSC subpopulations were indicated by single markers CD133+, CD15+, Sox2+ as well as co-expression of these markers CD133+Sox2+, CD15+Sox2+, or CD133+CD15+ compartments. The control group (DMSO) received DMSO. Error bars denote S.E.M. P: *P<0.05, **P<0.01, ***P<0.001, one-way analysis of variance.

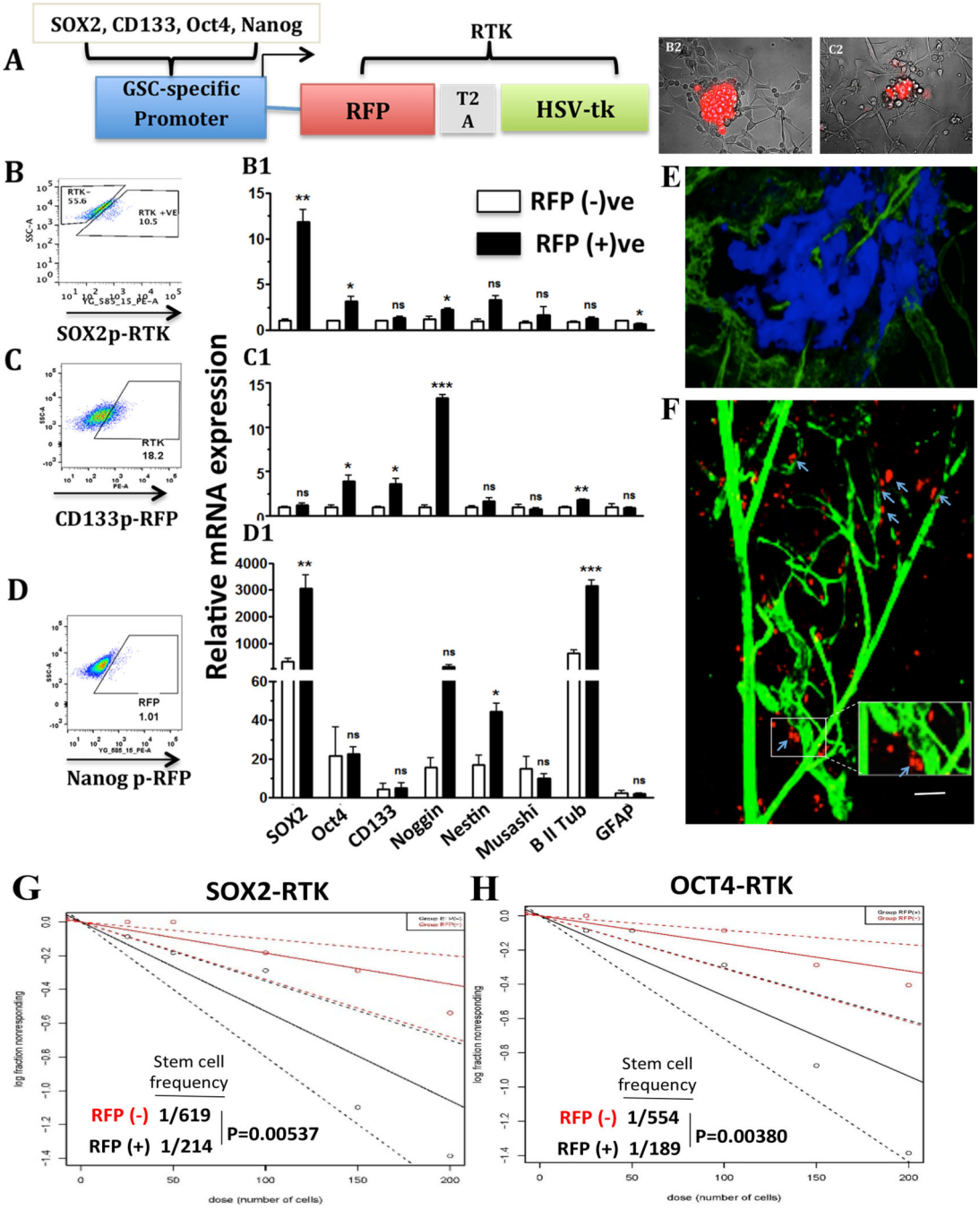

Figure 2. Development and validation of the GSC-specific reporter system

A) Schematic diagram of a GSC-specific reporter system, which was used to monitor cellular plasticity on a single-cell level. The Sox2, Oct4, Nanog, or CD133 promoters were inserted, each separately, into a lentiviral vector upstream of red fluorescent protein (RFP). B–D) U251 cells stably modified with different reporter systems were FACS sorted for the RFP-positive and the RFP negative cells and subject to real-time quantitative PCR analysis of the expression of the stemness genes (B1–D1). B2–C2) Neurosphere Assay performed with U251 cells expressing the Sox2-promoter reporter construct (Left) and the Nanog-

promoter reporter (right). The assay was conducted in Neural Basal media enriched with factors EGF and FGF using coated flasks, which allowed observation of both cell adhesion and neurosphere formation in the same assay. E) Intravital microscopy showing that within 2.5 weeks post implantation of intracranial BFP labeled GBM43-Sox2p-RFP tumor showing the image of the BFP-positive tumor area. F) the majority of the RFP-positive GSCs were localized near to the vasculature that is also known as peri vasculature niche (labeled with green dextran). G–H) Neurosphere Assay conducted with the sorted RFP-positive and negative cells from the GBM43-Sox2p-RFP (RTK) and U251-Oct4p-RFP (RTK) demonstrating RFP-positive cells with much higher cell renewing capacity. Error bars denote S.E.M. P: *P<0.05, **P<0.01, ***P<0.001, one-way analysis of variance.

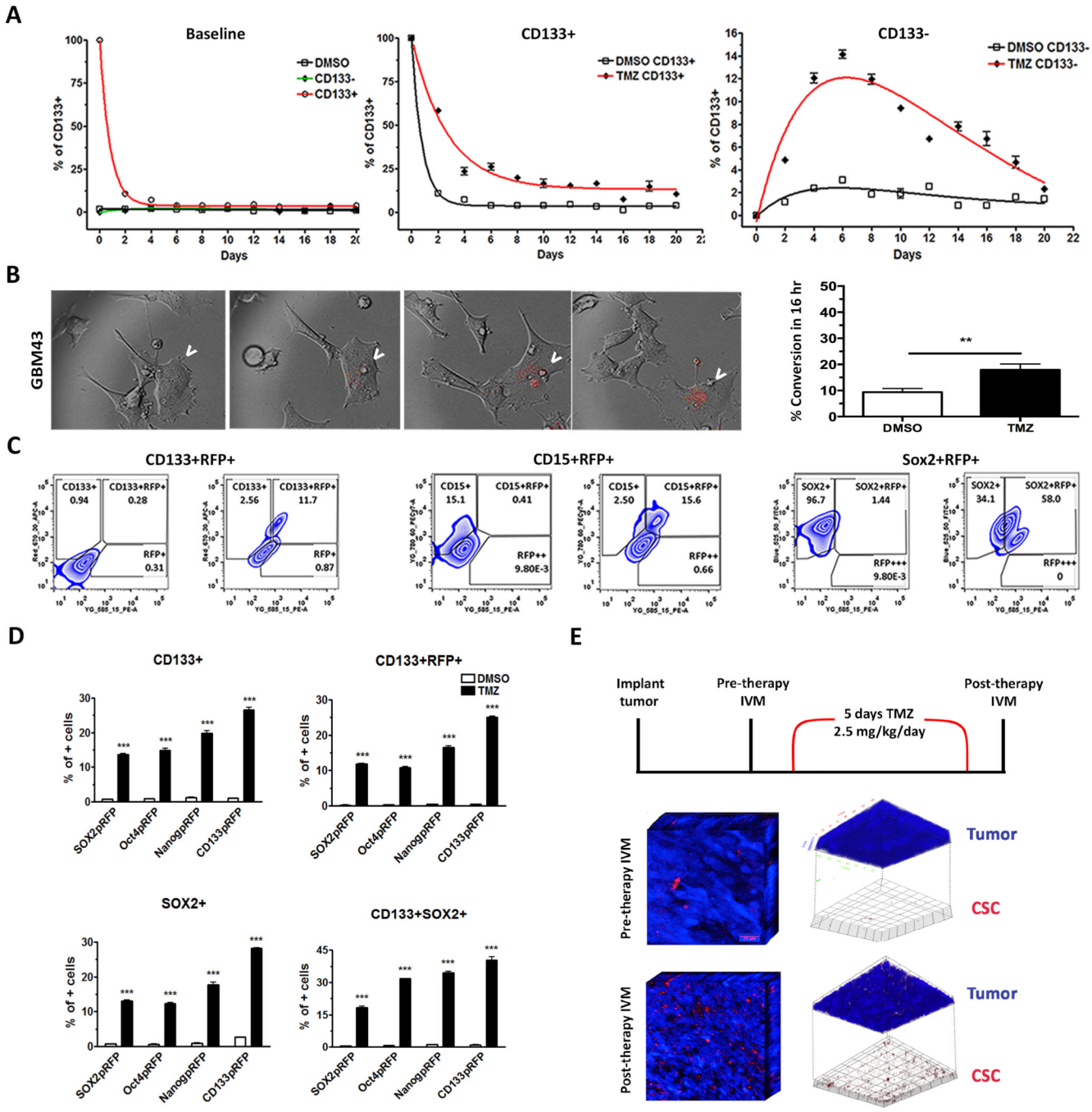

Figure 3. GSC-specific reporter systems faithfully monitor the GSC subpopulation in real time

A) Cell fate equilibrium pre- and post-sorting for CD133+/− populations throughout the course of 20 days (left). The GBM43 PDX line was cultured with or without 50μM TMZ in the 10% FBS differentiation condition media, and FACS-sorted out stem-like CD133+ and non-stem CD133− subpopulations of each group. The Dynamics of equilibrium-state for each population was monitored by FACS analysis of the CD133+ cells over 20 days. B) Real-time microscopy images of a single cell undergoing activation of CSC-specific promoters as a representation of conversion from non-GSC to a stem-like state after

treatment with TMZ in the GBM43 PDX model, visualized by the RFP and indicated by the arrows. Left, Graph depicting the increased frequency of conversion events when treating with TMZ as compared to control. The control group (DMSO) received DMSO. C) Zebra plots (flow cytometry) of the Sox2-RFP reporter system with and without TMZ (50μM) looking at CD133, CD15, and Sox2 co-expression with RFP. D) The GBM cells stably expressing CSC-specific promoter driven RFP reporter gene cultured with TMZ for 8 days. Percentages of cells expressing CD133+RFP+, CD133, CD15, Sox2, CD133+CD15+, or CD133+Sox2+ analyzed by FACS after 8 days post-TMZ therapy as compared to DMSO control. E) 3D representation of a tumor pre- and post-chemotherapy in vivo. GBM43 blue-tagged cells modified with Oct4-RFP lentivirus were implanted subcutaneously, and images were taken using intravital microscopy pre- and post-TMZ therapy (left). Tumors post-therapy show increased RFP expression scattered throughout the tumor burden (middle). Upon analysis of signal intensity, CSCs can be isolated out of the tumor, further highlighting the increase in the frequency of CSCs post-therapy, indicated by RFP expression (right). Error bars denote S.E.M. P: ns ($P>0.05$), *$P<0.05$, **$P<0.01$, one-way analysis of variance.

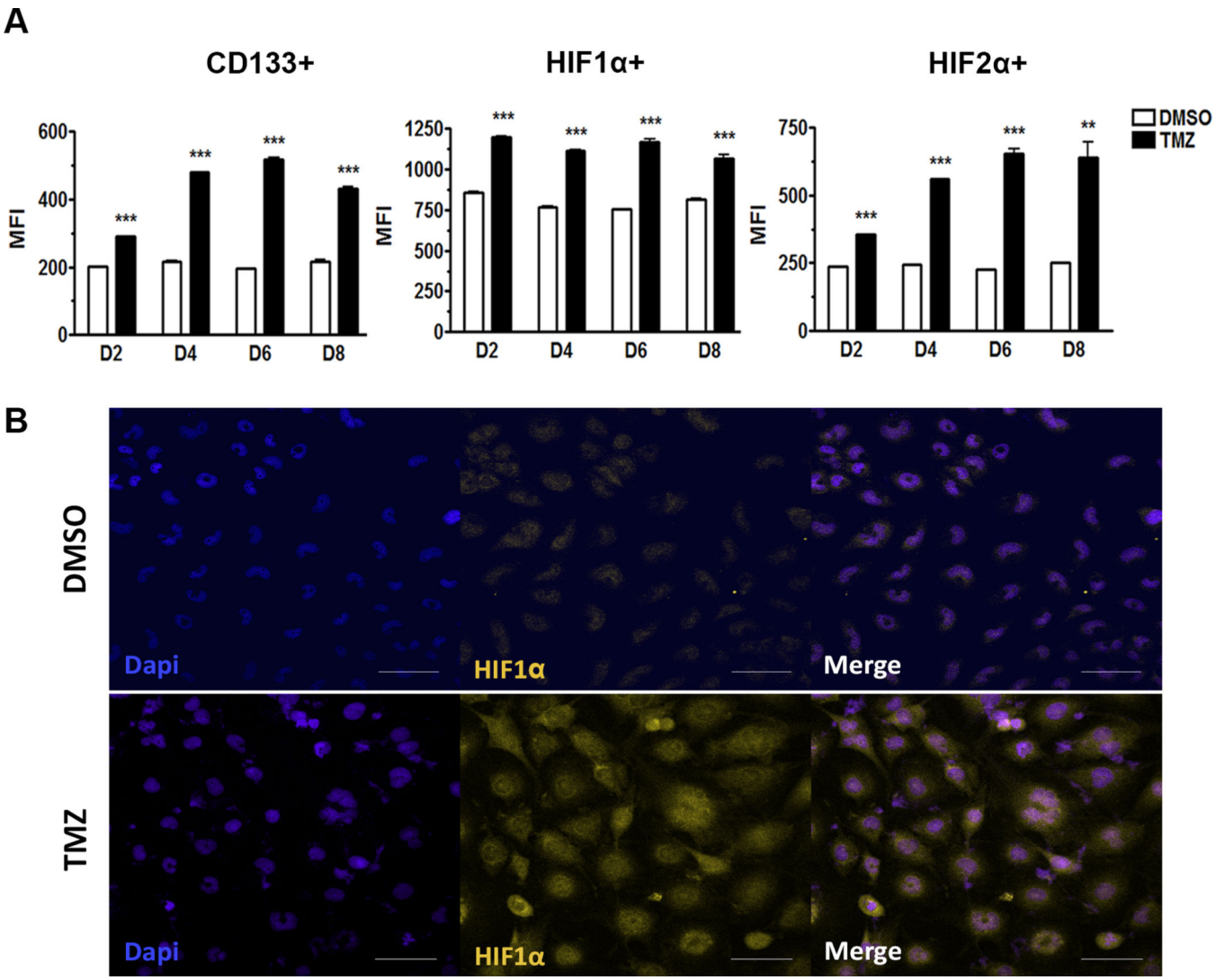

Figure 4. HIF1α and HIF2α are upregulated upon primary chemotherapy in the recurrent model

A) Flow cytometry analysis of GBM43 cells treated with TMZ (50μM) 2–8 days post-treatment. CD133 shows a peak at day six, HIF1α expression increases at day two and remains at similar levels throughout, and HIF2α also shows a peak at day six, all post-therapy. B) Immunofluorescence analysis of GBM43 line treated with TMZ (50μM) for 48 hours demonstrating induction of HIF1α post therapy. The control group (DMSO) received DMSO. Error bars denote S.E.M. *P: **P<0.01, ***P<0.001,* one-way analysis of variance.

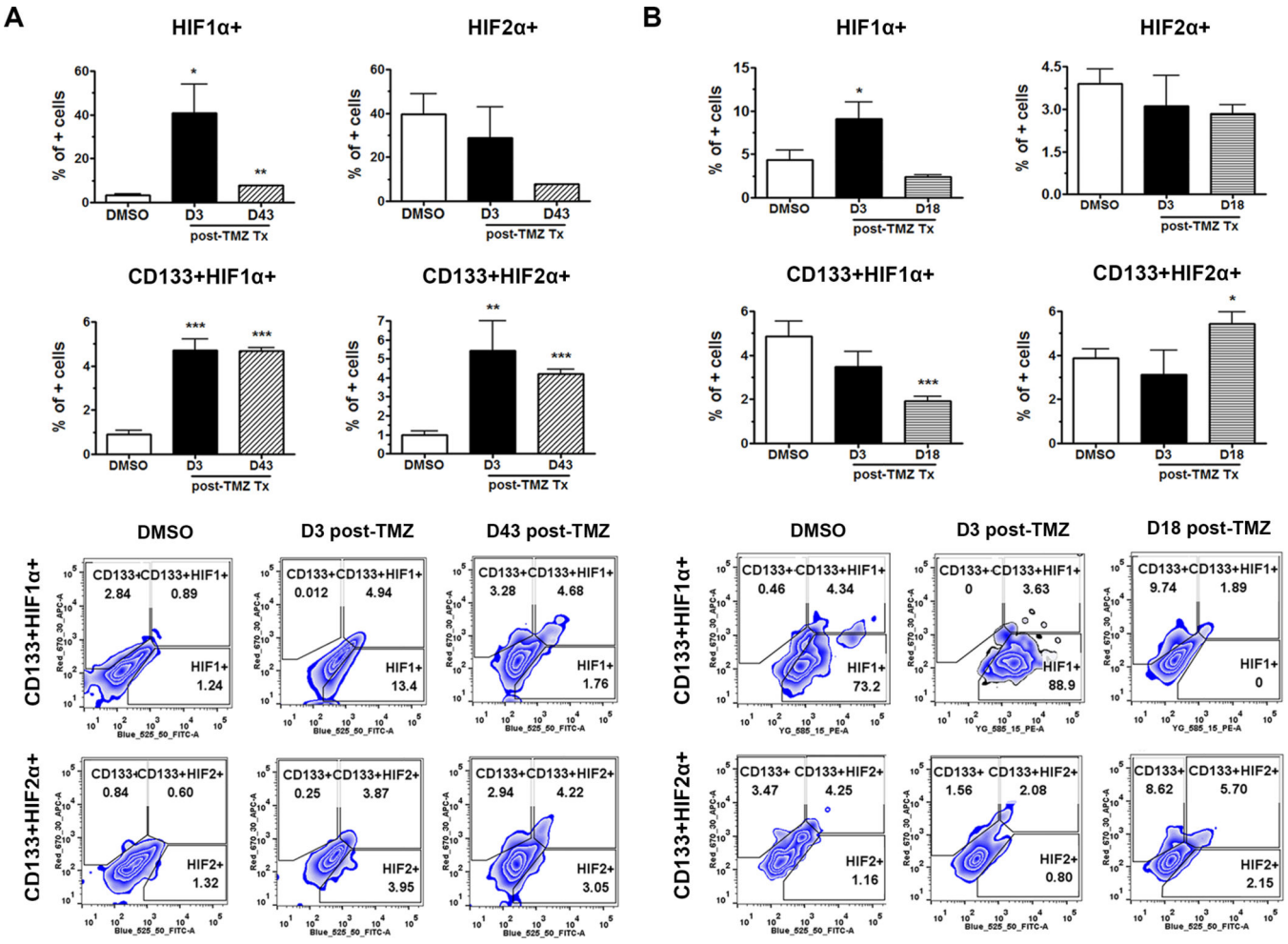

Figure 5. Dynamics of HIF1α and HIF2α expression in the recurrent model

A,B) The BFP+ PDX lines were implanted orthotopically and waited for xenograft establishment. A dose of 2.5 mg/kg/day of TMZ was administering intraperitoneally for 5 days in tumor-bearing mice. The HIF1α and HIF2α expression, as well as their localization within the CD133+ PDX GBM cells, were examined by FACS analyzing only the BFP positive cellular compartment in the brain. There is overall greater expression of HIF1α immediately post-treatment in both GBM6 (A) and GBM43 (B) PDX models. HIF2α activity presents itself in a more delayed manner, i.e. D43 and D18 post-treatment, represented by the CD133+HIF2α + compartment. The control group (DMSO) received DMSO. Error bars denote S.E.M. P: *P<0.05, **P<0.01, ***P<0.001, one-way analysis of variance.

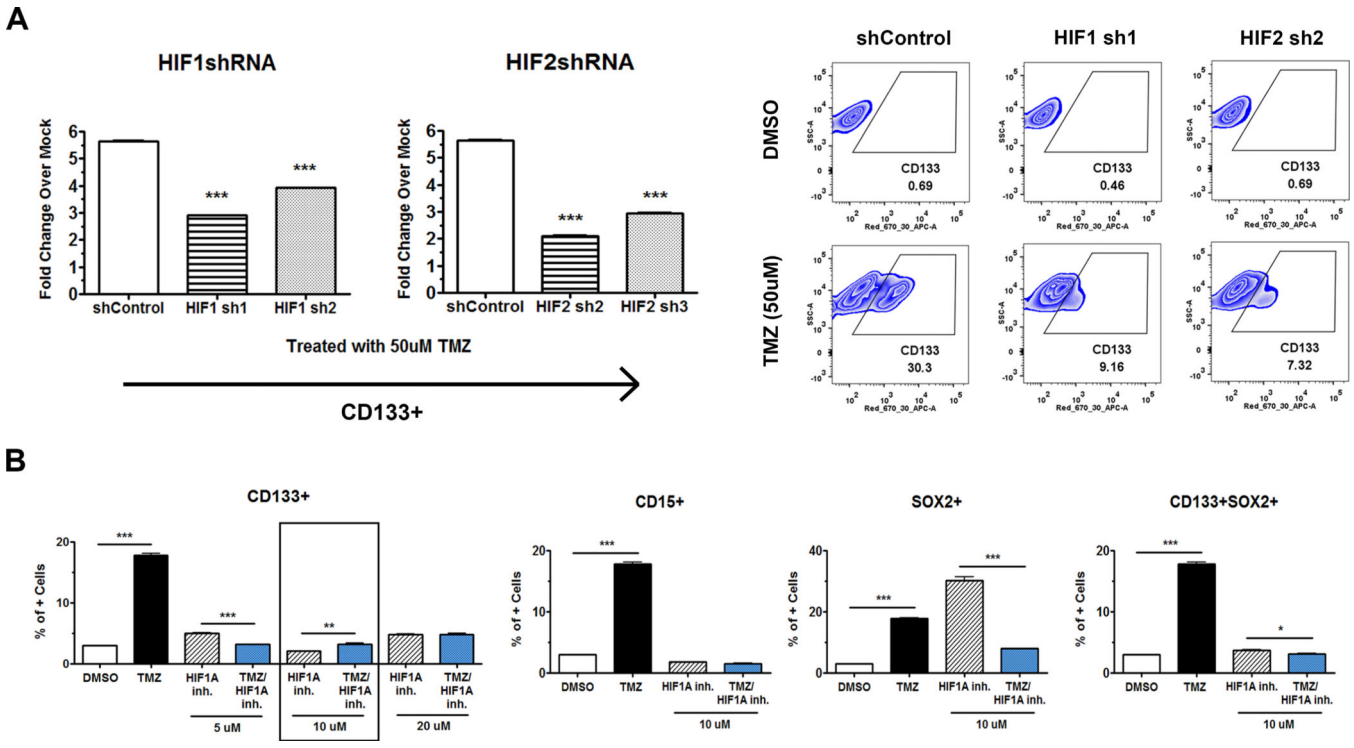

Figure 6. HIF-mediates the conversion of non-GSCs into GSCs

By eliminating HIF1α and HIF2α expressions, we can prevent cells from converting into stem-like states, identified by GSC markers. A) Knockdown of HIF1α and HIF2α using the respective shRNA shows that after primary TMZ therapy, there is attenuated CD133 expression as compared to the shRNA vector control. Data was expressed fold change for CD133+ GSC population over DMSO-treated control. On the right panel representative FACS plot for HIF knockdown cells. B) Application of an HIF translation inhibitor (10μM) one time in combination with TMZ completely prevents the conversion from non-GSCs to GSCs after 8 days post therapy, according to CD133+, CD15+, Sox2+, CD133+Sox2+, and CD133+CD15+ expressions after TMZ therapy. The control group (DMSO) received DMSO. Error bars denote S.E.M. P: *P<0.05, **P<0.01, ***P<0.001, one-way analysis of variance.